frontiers | Frontiers in Materials

TYPE Original Research
PUBLISHED 08 December 2022
DOI 10.3389/fmats.2022.1044495



OPEN ACCESS

EDITED BY
Mehdi Derradji,
Ecole Militaire Polytechnique (EMP), Algeria

REVIEWED BY
Mohamed El-Aassar,
Jouf University, Saudi Arabia
Semra Akgönüllü,
Hacettepe University, Turkey

*CORRESPONDENCE
Jorge R. Kawas,
jorge.kawasgr@uanl.edu.mx
Sara Paola Hernández-Martínez,
sara.hernandezma@uanl.edu.mx

SPECIALTY SECTION
This article was submitted to Polymeric and Composite Materials, a section of the journal Frontiers in Materials

RECEIVED 14 September 2022
ACCEPTED 10 November 2022
PUBLISHED 08 December 2022

CITATION
Delgado-Cedeño A, Hernández-Martínez SP, Ramos-Zayas Y, Marroquín-Cardona AG, Méndez-Zamora G, Franco-Molina MA and Kawas JR (2022), Insoluble chitosan complex as a potential adsorbent for aflatoxin $B_1$ in poultry feed. *Front. Mater.* 9:1044495. doi: 10.3389/fmats.2022.1044495



# Insoluble chitosan complex as a potential adsorbent for aflatoxin $B_1$ in poultry feed

Armando Delgado-Cedeño[1], Sara Paola Hernández-Martínez[2,3]*, Yareellys Ramos-Zayas[1,3], Alicia Guadalupe Marroquín-Cardona[1], Gerardo Méndez-Zamora[1,2], Moisés Armides Franco-Molina[4] and Jorge R. Kawas[1,3]*

[1]Universidad Autónoma de Nuevo León, Posgrado Conjunto Agronomía-Veterinaria, Nuevo León, México, [2]Universidad Autónoma de Nuevo León, Facultad de Agronomía, Nuevo León, México, [3]MNA de México, Nuevo León, México, [4]Universidad Autónoma de Nuevo León, Facultad de Biología, Nuevo León, México

As a class of secondary metabolites or toxins produced by fungi, aflatoxins can poison humans and animals; among them, aflatoxin $B_1$ ($AFB_1$) is the most dangerous one owing to its carcinogenic and mutagenic properties that increase risks for hepatocellular carcinoma in humans; hence, adsorbents such as smectites are commonly included in poultry feed to mitigate their effects. In this study, chitosan was crosslinked with sodium dodecyl sulfate (SDS) to form an insoluble polymer complex that is stable at the relevant physiological pH levels. The characterization *via* Fourier transforms infrared spectroscopy revealed the interaction between the sulfate groups of the SDS and the amine group of chitosan (1,016 and 819 $cm^{-1}$); this result was further confirmed by the X-ray diffraction patterns with a change in the crystalline structure of the chitosan-insoluble complex ($2\theta$ = 4.76°, 7°, and 22°). The morphology of the chitosan-insoluble complex obtained using a field emission scanning electron microscope (FE-SEM) revealed that particles were slightly porous. After characterization, the performance of the chemically modified polymer complex was evaluated as an adsorbent for $AFB_1$ and compared with those of the unmodified chitosan, soluble chitosan complex, and commercial montmorillonite clay binder. In addition, the polymer complex was investigated as an adsorbent in an *in vitro* model for the poultry gastrointestinal system. Sequestration of $AFB_1$ by a chemically modified polymer complex was 93.4%, equivalent to that of commercial montmorillonite clay (99.5%). However, these treatments also sequestered microminerals, particularly selenium and iron. This pH-stable, high-capacity adsorbent could be used in poultry feed to reduce the uptake of $AFB_1$.

KEYWORDS

**chitosan, polymers, crosslinking, sodium dodecyl sulfate, aflatoxin $B_1$, *in vitro* poultry gastrointestinal model**

## Introduction

Mycotoxins are toxic compounds naturally produced by fungi such as *Aspergillus*, *Penicillium*, and *Fusarium* (Liew and Mohd-Redzwan, 2018). Among the hundreds of mycotoxins, the best-known ones are aflatoxins, ochratoxins, trichothecenes, zearalenone, fumonisins, and patulin (Omotayo et al., 2019). The aflatoxins are produced by the *Aspergillus* fungus species, which are considered potent hepatotoxins and carcinogens, that contaminate maize, peanuts, and cottonseed (Duan et al., 2019). More than 20 types of aflatoxins (AFs) exist in nature; the main ones are aflatoxin $B_1$ ($AFB_1$), $AFB_2$, $AFG_1$, $AFG_2$, and the secondary hydroxylated metabolites of $AFB_1$ and $AFB_2$, $AFM_1$ and $AFM_2$.

Studies in animals and humans (Centre International de Recherche Sur le Cancer, 2002) have shown that $AFM_1$ and $AFM_2$ are transferred to milk and meat (Tozzi et al., 2016; Kumar et al., 2017) and that $AFB_1$ is the most dangerous mycotoxin because it is adsorbed and metabolized in the liver by cytochrome P450 (CYP) enzymes into $AFB_1$-8,9-epoxide, which covalently binds to DNA, RNA, and proteins to induce carcinogenic and mutagenic effects (Yang et al., 2012; Patrick and Stepman, 2019; Kövesi et al., 2020). Hence, the International Agency for Research on Cancer indicated AFs as carcinogenic (Group 1) (Centre International de Recherche Sur le Cancer, 2002) because of increased risks for hepatocellular carcinoma in humans (Cogliano et al., 2011; Marchese et al., 2018).

The structure of AFs is composed of a bifuran ring fused to a coumarin nucleus with a pentanone ring (AFB and AFM) or a six-membered lactone ring in AFG. The four compounds produce fluorescence (B = blue, and G = green), which allows their detection (Dhanasekaran et al., 2011). The chromatographic and spectroscopic techniques are the most widely used methods for the detection of AFs, followed by enzyme-linked immunosorbent assays (ELISA), polymerase chain reaction (PCR), radioimmunoassay (RIA), immunoaffinity column assay, and chemiluminescence immunoassay (CLIA). However, these techniques have some limitations. Recently, biosensing techniques have been developed to increase the specificity, sensitivity, and accuracy of AFs detection. The biosensors consist of biorecognition elements such as immunoglobulins, enzymes, cells, molecularly imprinted polymers, or drugs. These elements have selectivity for the targeted analyte (Yadav et al., 2021). Akgönüllü et al. (2020) designed a nanosensor containing imprinted polymers with gold nanoparticles selective to $AFB_1$, with a limit of detection of 1.04 pg/ml in nuts and corn samples. Similarly, Salvador et al. (2022) developed an $AFB_1$ detection method based on the lateral flow immunoassay (LFIA). This test presented a limit of detection of 4.80 ng/ml in almond milk.

The Food and Drug Administration (FDA) established a level of 20 μg/kg of AFs for all foods, including animal feeds, to avoid and reduce danger to the health of animals or risk of poisoning humans that consume food derived from the exposed animals (Guidance for FDA, 2019). However, the effect of AFs level varies between species. Ducks, pigs, and dogs die immediately after exposure to AFs at higher concentrations, whereas humans, chickens, and rats are less vulnerable to acute poisoning. In the poultry species, ducks are the most sensitive to aflatoxins, followed by turkey poults, broilers, and laying hens (Patrick and Stepman, 2019). The acute effects lead to low productivity, susceptibility to disease, and contamination of eggs and meat (Razzaghi-Abyaneh, 2013; Fouad et al., 2019; Peles et al., 2019). Only ducks are known to develop cancer; however, owing to their short lifespan, the acute effects in ducks are still critical (Diaz and Murcia, 2019).

In the case of chickens, chicks are more susceptible to AFs exposure than adults, males being the most affected owing to their high growth rate. The major negative effects of AFs are decreased growth rate, poor feed conversion, anemia, immunosuppression, more susceptibility to infectious disease, lower egg production, and embryonic mortality (Ochieng et al., 2021).

Prevention of AFs production reduces the contamination of feeds. Antifungal agents, UV, X-rays or microwave irradiation, thermal inactivation, decontamination with ozone ($O_3$), and chemical compounds (acids, salts, oxidants, reducing agents) can be used to eliminate or decrease $AFB_1$, and the use of adsorbents can prevent $AFB_1$ from entering the intestinal tract after ingestion (Patrick and Stepman, 2019; Su, 2020).

Kurup et al. (2022) reported that the use of UV-A light reduced the concentration of $AFB_1$ and $AFM_1$ in milk, and in *in vitro* model with HepG2 cells, they observed that UV-A light decreased the aflatoxins-induced cytotoxicity. McKenzie et al. (1998) evaluated the capability of ozone ($O_3$) to degrade $AFB_1$ in contaminated whole kernel corn, obtaining a reduction of 95% in $AFB_1$ concentration. Furthermore, corn-fed turkeys treated with $O_3$ did not show changes in organ weight, liver discoloration, serum enzyme activity, hematological parameters, and blood chemistry, in contrast to corn-fed turkeys with $AFB_1$ and without $O_3$.

Wang et al. (2022) reported that the use of natural antioxidants can reduce the effects of AFs, such as oxidative stress, cytotoxicity, and DNA damage. *In vitro* and *in vivo* studies demonstrated that the use of curcumin, a polyphenolic molecule extracted from the *Curcuma longa* (turmeric), inactivated CYP450 enzymes preventing mitochondrial malfunction, apoptosis, inflammatory response, modification of autophagy, and gut microbiome but allowed free radical scavenging and downregulation of oxidative stress effects produced by $AFB_1$ (Dai et al., 2022). Similarly, resveratrol, a polyphenolic phytoalexin present in grapes, berries, peanut skins, and other plant parts, reduced reactive oxygen species (ROS) and prevented the $AFB_1$-induced testicular damage in *in vivo* studies (Omur et al., 2019; Wu et al., 2020); in *in vitro* study, it reduced $AFB_1$ induced cytotoxicity and reverted transcriptional modification induced by

$AFB_1$ (Pauletto et al., 2021). Other molecules such as vitamin E and selenium have been demonstrated to reduce the negative effects of mycotoxins in swine, poultry, and ducks (Neeff et al., 2018; Wu et al., 2021).

Another method for detoxification of $AFB_1$, is the use of adsorbents in animal feed, in which AFs bind to the adsorbent surface and are subsequently removed from the gastrointestinal tract (GT), instead of passing into the blood (Peles et al., 2019). Clay minerals, which are phyllosilicates characterized by layered structures consisting of tetrahedral sheets of silicon oxides with alternating octahedral sheets of aluminum oxide, are the most widely used adsorbents (Bibi et al., 2016; Speight, 2020). Based on the number of tetrahedral and octahedral sheets and their arrangement, clays of the smectites family can be classified as montmorillonite, beidellite, nontronite, saponite, and hectorite (Kumari and Mohan, 2021). These are differentiated by variations in chemical compositions involving substitutions of ions in tetrahedral (aluminum and silica) and octahedral cationic sites (aluminum, iron, magnesium, and lithium) (Odom, 1984). The cationic sites present in smectites allow the adsorption of $AFB_1$ by cation exchange and intercalation between the layers (Prasad et al., 2019; Núnez-Delgado, 2021).

Researchers have also considered various organic binders, such as yeast cell walls and lactic acid bacteria (Kim et al., 2019; Luo et al., 2020), β-D-glucans, chitosan, cellulose (El-Naggar and Thabit, 2014; Sid et al., 2021), and plant derivatives (Zavala-Franco et al., 2018; de Jesús Nava-Ramírez et al., 2021). Chitin is one of the most abundant biopolymers obtained from the exoskeleton of crustacea, insects, algae, and the cell wall of fungi (Aranaz et al., 2021). Chitosan is derived from deacetylated chitin, and it is formed by D-glucosamine and N-acetyl- D-glucosamine units linked by the β-1,4 glycosidic bonds (Muxika et al., 2017). Since chitosan is a nontoxic, biocompatible, and biodegradable polymer, it is commonly used in medicines for drug delivery systems, antimicrobials, wound dressing, and as an antioxidant (Zhao et al., 2018).

In agriculture, chitosan has been used as a protector against diseases and plagues, as well as to enhance the development and regulation of plant growth. Zachetti et al. (2019) reported that chitosan reduces growth rates of *Fusarium graminearum*, *Fusarium verticillioides*, and *Fusarium proliferatum*, as well as the concentration of deoxynivalenol (DON) and fumonisin (FB) in corn and wheat grain samples. Similarly, Cortés-Higareda et al. (2019) and Segura-Palacios et al. (2021) observed a decrease in AFs concentration in *Aspergillus flavus* treated with chitosan *in vitro*.

The use of chitosan as an adsorbent for mycotoxins was reported by Solís-Cruz et al. (2017) and Abbasi Pirouz et al. (2020), who observed that this molecule can adsorb $AFB_1$. Zhao et al. (2015) observed that the capacity of adsorption increased in chitosan crosslinked with other molecules. Additionally, the use of chitosan as an additive in poultry feed demonstrates positive impacts on productive parameters, immune responses, and antioxidant capacity (Swiatkiewicz et al., 2015). Further, chitosan can be used as an alternative to antibiotics with an improvement of gut (Nuengjamnong and Angkanaporn, 2018; Osho and Adeola, 2019) and liver function (Chang et al., 2020).

When chitosan is in an acidic medium, the amine groups of D-glucosamine units are protonated, and the resultant cationic polymer easily interacts with diverse molecules (Worthen et al., 2019). Furthermore, the hydroxyl (OH) and amine ($NH_2$) groups can be chemically modified to improve the physical and chemical properties of the polymer (Wang et al., 2020), including the affinity for anions and cations. The SDS forms a complex with chitosan (Petrovic et al., 2016) that features numerous adsorption sites and a flexible polymer chain structure (Vakili et al., 2019). SDS is a surfactant comprising a hydrophobic carbon chain ($C_{12}$) and a polar sulfate head capable of interacting with positively charged molecules (Li and Ishiguro, 2016; Jafari et al., 2018). The sulfonate and sulfate groups of SDS interact electrostatically with the $NH_2$ groups of the D-glucosamine unit of chitosan, forming an insoluble complex that can bind anionic organic molecules and contaminants, such as heavy metals and dyes (Chiappisi and Gradzielski, 2015). The chitosan-SDS complex has previously been used as an adsorbent for heavy metals in water (Bat-Amgalan et al., 2021); however, there are no studies on the use of the chitosan–SDS complex as an $AFB_1$ adsorbent.

To the best of our knowledge, no studies have been reported on the use of modified chitosan as a mycotoxin binder; therefore, this study aimed to synthesize chitosan crosslinked with SDS surfactant to increase the adsorption capacity of chitosan for $AFB_1$, maintaining the stability of the molecule at different pH values in an *in vitro* model for poultry. $AFB_1$ adsorption on the resultant insoluble complex was compared with that of the unmodified chitosan, soluble chitosan complex, and commercial montmorillonite clay, as a control experiment. The insoluble complex and the other treatments were further tested for micromineral removal.

# Materials and methods

## Reagents

The following reagents and chemicals were purchased from Sigma Aldrich (Burlington, MA, United States): $AFB_1$ from *Aspergillus flavus* (catalog no. A6636), pepsin from porcine gastric mucosa (catalog no. P7000), pancreatin from porcine pancreas (catalog no. P7545), chitosan (medium molecular weight, 75%–85% deacetylated, catalog no. 448877), and SDS (catalog no. 436143). Acetonitrile (catalog no. 75-05-8), methanol (catalog no. 67-56-1), and water (catalog no. 7732-18-5) were purchased from Fisher Scientific (Waltham, MA, United States). Sources of the inorganic microminerals required, such as iron sulfate, manganese sulfate, zinc sulfate, and sodium sulfate, were provided by MNA de México (Nuevo León, México).

TABLE 1 Nutritional requirements minerals for poultry.

| Trace mineral source | Concentration of mineral (mg/500 ml) |
|---|---|
| Iron sulfate | 33.33 |
| Manganese sulfate | 184.62 |
| Zinc sulfate | 151.52 |
| Sodium selenite | 0.33 |

## Synthesis of chitosan-based adsorbents

First, a soluble chitosan complex (chitosan-soluble) was prepared by mixing chitosan (2% w/v) with an acetic acid solution (0.1 M), followed by adding NaOH (2 M) and stirring for 20 min at 300 rpm. The formed precipitate was washed thrice with distilled water and dried at 60°C for 24 h. To obtain the insoluble chitosan complex (chitosan-insoluble), 2 g of chitosan-soluble was dissolved in an acetic acid solution (0.1 M) under magnetic stirring for 1 h at 400 rpm. The solution was then mixed with an SDS solution in Milli-Q water (0.6% w/v). The obtained beads were washed thrice with distilled water and dried at 60°C for 24 h. Both chitosan-soluble and chitosan-insoluble complexes were ground and sieved to use as aflatoxin adsorbents and were compared with a commercial montmorillonite clay (Toxisorb™ Premium, Clariant; Puebla, México).

## Adsorbent characterization

The functional groups of the adsorbents chitosan, chitosan-soluble, chitosan-insoluble complexes and commercial montmorillonite clay, commercial montmorillonite clay, and their interactions with $AFB_1$ were determined using attenuated total reflection (ATR) Fourier transform infrared (FTIR) spectroscopy. The adsorbent was placed onto a diamond ATR crystal, and the spectra were recorded using an FTIR spectrometer (Perkin Elmer; Waltham, MA, United States) based on 16 accumulated scans at a resolution of 4 $cm^{-1}$ between 4500 and 500 $cm^{-1}$. Data were analyzed using the Spectrum 10 software (Perkin Elmer). The adsorbents (chitosan, chitosan-soluble, and chitosan-insoluble complexes) were characterized using X-ray diffraction (XRD) in a Dmax2100 (Rigaku, Tokyo, Japan), and the Cu Kα radiation (1.5406 Å) was determined at 20 mA and 30 kV. The morphology and structure of adsorbents were characterized using an ultra-high resolution field emission scanning electron microscope (UHR FE-SEM, Hitachi SU8020; Schaumburg, IL, United States). Before analysis, the samples (chitosan complexes) were coated with a gold layer and the images were taken at an acceleration voltage of 3 kV for the chitosan complex and 1 kV for commercial montmorillonite clay at 500x magnification.

## pH-dependent adsorption of $AFB_1$

The adsorption percentage of $ABF_1$ was determined according to the literature (Marroquín-Cardona et al., 2009). A stock solution of $AFB_1$ (5,000 μg/2 ml) was prepared in acetonitrile and further diluted with distilled water to a concentration of 4 μg/ml. The UV absorption of the solutions was measured at 364 nm using a UV-visible spectrophotometer (Shimadzu UV-1601PC; Midland, ON, Canada). For the adsorption experiment, 40 mg of the adsorbent was weighed and mixed with the $AFB_1$ solution (4 μg/ml, 1 ml) and water (4 ml) to reach a final $AFB_1$ concentration of 0.8 μg/ml, and the pH was adjusted to 2.5, 5.2, or 6.6. There were also two sets of control samples: 1) water at pH 2.5, 5.2, and 6.6 with $AFB_1$ but no adsorbent and 2) water at pH 2.5, 5.2, and 6.6 with the adsorbent but no $AFB_1$. The mixture of the solution and adsorbent was incubated at 40°C for 45 min under constant agitation. Finally, the samples were centrifuged at 2,000 rpm for 20 min, and the absorbance of the supernatant was measured at 364 nm using the aforementioned UV-visible spectrophotometer. All measurements were performed in quadruplicate, and the adsorption percentage of $AFB_1$ was obtained by the difference between the initial and final $AFB_1$ concentrations in the supernatant using the following equation (Solís-Cruz et al., 2017):

$$Adsorption\,\% = (Ci - Cf)/Ci \times 100 \quad (1)$$

where *Ci* and *Cf* are the initial and final concentrations of $AFB_1$ (μg/ml) in the supernatant, respectively.

## Quantification of $AFB_1$ *via* ultra-performance liquid chromatography (UPLC) after adsorption in an *in vitro* gastrointestinal model for poultry

An *in vitro* gastrointestinal model for poultry was previously designed to corroborate the efficiency of the adsorbents in poultry feed (Solís-Cruz et al., 2017). The model simulates three parts: 1) the crop (pH 5.2, constant agitation and incubation at 40°C for 30 min); 2) the proventriculus (pH 2.5, 3,000 U pepsin under constant agitation, and incubation at 40°C for 45 min); and 3) the small intestine (pH 6.6, 6.84 mg pancreatin under constant agitation, and incubation at 40°C for 2 h). After incubation, the mixture was centrifuged at 2,000 rpm for 10 min. The supernatant was passed through a 0.2 μm syringe filter (Wathman® UNIFLO® 25; Burlington, MA, United States), evaporated at 50°C under a nitrogen stream, and the obtained residue was dissolved in 500 μl of the mobile phase (6.4:1.8:1.8 water/methanol/acetonitrile). The dissolved sample was then analyzed in an ACQUITY UPLC® H-Class Bio System (Waters, Milford, MA, United States), coupled with a fluorescence detector and an ACQUITY UPLC

BEH C18 reversed phase column (2.1 mm × 50 mm, 1.7 μm). The liquid sample (10 μl) was injected and eluted with the aforementioned mobile phase at a flow rate of 0.5 ml/min and detected at $\lambda_{ex}/\lambda_{em}$ = 365 nm/429 nm. $AFB_1$ was identified by its retention time (4 min) and compared to a pure $AFB_1$ standard solution (200 ng/ml).

Each sample was measured in quadruplicate. The $AFB_1$ concentration in the mobile phase was determined using a pre-determined calibration curve with $R^2$ = 0.996 (for details see Supplementary Table S1; Supplementary Figure S1, S2). The percentage of adsorbed $AFB_1$ was calculated from the difference in the peak area between samples with and without the adsorbent using the following equation (Wang et al., 2018):

$$R = (1–A1/A0) \times 100 \quad (2)$$

where *A0* and *A1* are the peak area without and with the adsorbent, respectively.

## Micromineral adsorption percentage

The adsorption percentage of microminerals (iron, manganese, zinc, and selenium) was measured using a standard solution that contained the mineral amounts nutritionally required by poultry (Table 1) (Ross Broiler: Nutrition Specifications, 2019). The micromineral inorganic sources were dissolved in 500 ml of distilled water and 40 mg of chitosan, chitosan-soluble, chitosan-insoluble, or commercial montmorillonite clay were weighed and mixed with 6 ml of the micromineral solution. The samples were incubated under conditions simulating an *in vitro* gastrointestinal poultry model and were centrifuged at 2,000 rpm for 20 min. Finally, the concentrations of the microminerals in the supernatant were determined by inductively coupled plasma-optical emission spectroscopy (ICP-OES; Perkin Elmer OPTIMA 2000 DV).

## Statistical analysis

The experimental data were analyzed in a completely randomized design using Statistics 9 Analytical Software (Tallahassee, FL, United States). The data were subjected to a one-way analysis of variance, and the means were compared using Dunnett´s test at $p \leq 0.05$.

# Results

## Adsorbent characterization *via* infrared spectroscopy

FTIR spectra were used to determine the chemical composition of the complexes and their interaction with $AFB_1$. Figure 1 shows the FTIR spectra of chitosan, chitosan-soluble, chitosan-insoluble, and commercial montmorillonite clay, with and without adsorbed $AFB_1$. The spectrum of pure chitosan (Figure 1A) displays a characteristic band at 3,268 $cm^{-1}$ for hydroxyl group (OH) stretching; two bands at 2,930 and 2,875 $cm^{-1}$ for C–H stretching; and strong bands at 1,637, 1,533, and 1,408 $cm^{-1}$ for C = O stretching (amine I), N–H bending, and C–H stretching, respectively. Another strong band at 1,016 $cm^{-1}$ can be attributed to the stretching vibrations of characteristic groups of the polymer (–C–O–C–), and the band at 903 $cm^{-1}$ corresponds to the amine group ($NH_2$). In the spectrum of chitosan-soluble (Figure 1B), the characteristic absorption bands of chitosan are shifted and have lower intensities. The spectrum of CH-insoluble (Figure 1C) also shows characteristic bands of chitosan at 3,416–1,470 $cm^{-1}$, along with additional bands at 1,212, 1,055, 1,016, 819, and 630 $cm^{-1}$ due to the insertion of sulfate groups (S=O, R–O–S, and S–O) into the chitosan molecule. The FTIR spectra also show that $AFB_1$ interacts with the amine groups of chitosan and chitosan-soluble (Figure 1E and Figures 1F, respectively). Chitosan-insoluble also exhibits interaction between the amine and sulfate groups (Figure 1G). Finally, the main functional groups of montmorillonites were observed in the FTIR spectrum of commercial clay (Figure 1D); vibrational band at 1,637 $cm^{-1}$ corresponded to H-O-H bending of water, bands at 798 and 693 $cm^{-1}$ corresponded to stretching vibrations of Si-O, and band at 515 $cm^{-1}$ corresponded to bending vibration of Al-O. The interaction of $AFB_1$ with montmorillonite clay was observed with Si-O and Al-O groups (Figure 1H).

XRD was used to identify the crystallinity, and physical properties of chitosan, chitosan-soluble, and chitosan-insoluble complexes. The XRD patterns of chitosan complex are shown in Figure 2, where the chitosan exhibited two peaks at 2θ = 9.52° and 19.8°, consistent with the crystalline structure of chitosan. However, the intensity of these peaks decreased in the diffraction patterns of chitosan-soluble and chitosan-insoluble complexes. Besides, the chitosan-soluble complex exhibited new peaks at 2θ = 16.7°, 18.6°, 37.9°, 40.5°, 45°, 52.9°, and 57.2°. Similarly, chitosan-insoluble complex exhibited new peaks at 2θ = 4.7°, 7°, 11.6°, 19.1°, 22°, and 29.9°, indicating changes in the crystalline structure.

The surface structure and morphology of adsorbents were observed using SEM analysis. Figure 3 shows micrographs representative of the adsorbents morphology where the chitosan shows nonporous flakes (10–90 μm). Similarly, chitosan-soluble flakes were porous (8–200 μm). However, the chitosan-insoluble dense particles were slightly porous (1–50 μm), and the commercial montmorillonite clay had porous particles (3–10 μm) and aggregates (30–60 μm).

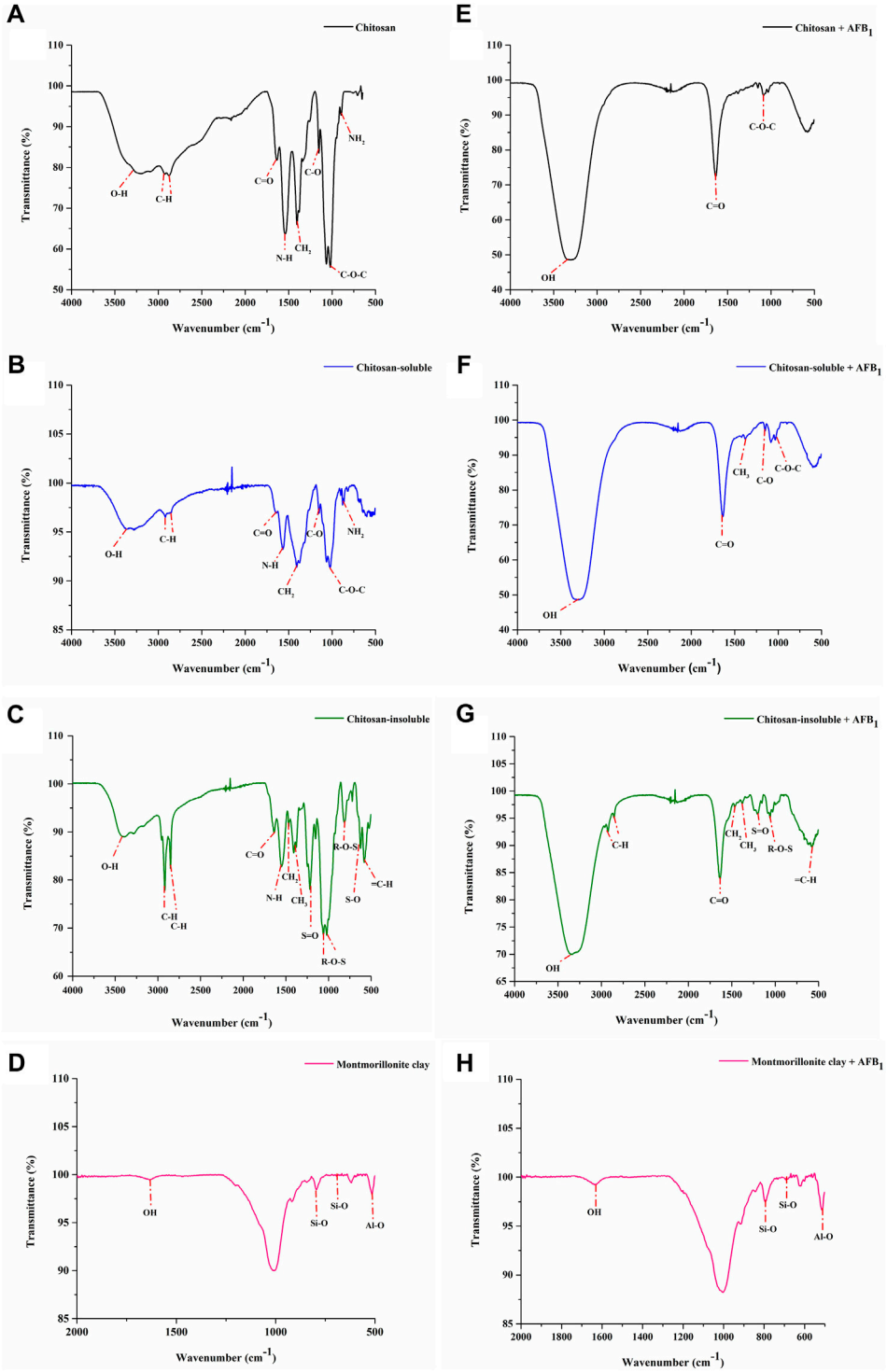


FIGURE 1
FTIR spectra: **(A)** chitosan, **(B)** chitosan-soluble, **(C)** chitosan-insoluble, **(D)** montmorillonite clay, and the interaction of $AFB_1$ with chitosan **(E)**, with chitosan-soluble **(F)**, with chitosan-insoluble **(G)**, and with montmorillonite clay **(H)**.

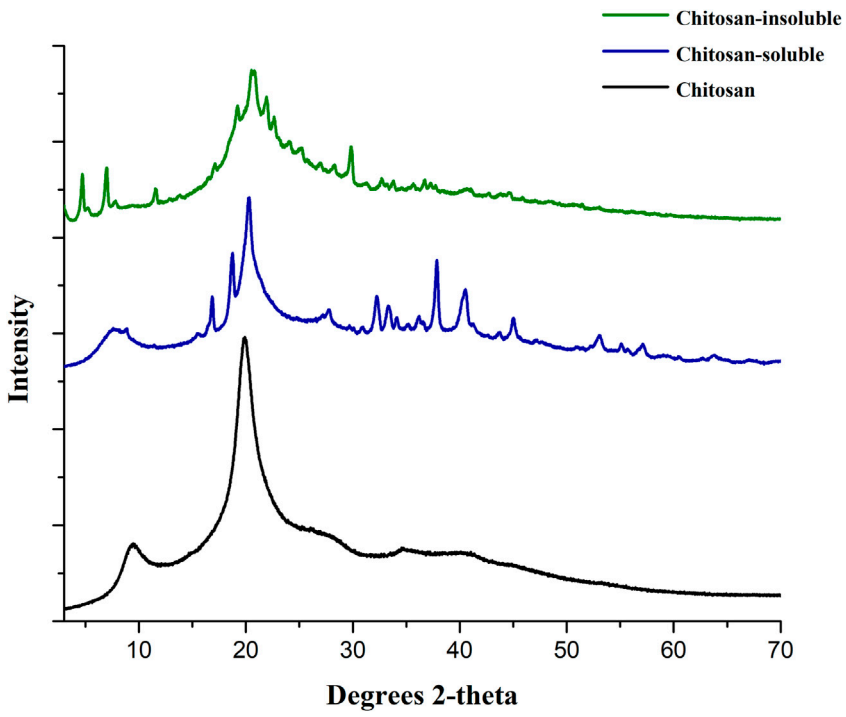


FIGURE 2
X-ray diffraction patterns (XRD) of chitosan, chitosan-soluble, and chitosan-insoluble.

## pH-dependent adsorption of $AFB_1$

Table 2; Figure 4 compare the $AFB_1$ adsorption percentages at different pH levels. At pH 5.2, the commercial montmorillonite clay (99.40% ± 1.03) and chitosan-soluble (96.43% ± 4.72) showed a higher adsorption ratio ($p$ = 0.001) compared to that of the chitosan-insoluble (79.17% ± 5.15) and chitosan (17.88% ± 1.89). In contrast, at pH 2.5, the commercial montmorillonite clay (95.83% ± 1.03), showed the highest adsorption ratio ($p$ = 0.001) followed by chitosan-insoluble (72.03% ± 2.53), chitosan-soluble (38.71% ± 4.44) and chitosan (1.81% ± 0.01). The same trend was observed at pH 6.6, the commercial montmorillonite clay ($p$ = 0.01) (82.14% ± 3.40) > chitosan-insoluble (75.60% ± 3.08) > chitosan-soluble (61.32% ± 2.32) > chitosan (13.05% ± 2.30).

## Quantification of $AFB_1$ *via* UPLC in an *in vitro* gastrointestinal model for poultry

From the UPLC chromatogram, $AFB_1$ was detected at a retention time of 4 min after adsorption on chitosan in the *in vitro* model (Figure 5A). The amount of $AFB_1$ in the supernatant decreased for chitosan-soluble complex (Figure 5B), and it was undetected for chitosan-insoluble complex (Figure 5C) and commercial montmorillonite clay (Figure 5D). From these data, $AFB_1$ adsorption in the *in vitro* model was the highest ($p$ = 0.0001) on commercial montmorillonite clay (199.06% ± 0.064; 99.52%), and chitosan-insoluble complex (184.98 ± 0.989 ng/ml; 93.44%), followed by the chitosan-soluble complex (129.6 ± 0.433 ng/ml; 64.79%) and chitosan (117.83 ± 0.668 ng/ml; 58.91%) (Table 3; Figure 6).

## Micromineral adsorption in an *in vitro* gastrointestinal model for poultry

The adsorptions of manganese (95.0% ± 2.30) and selenium (90.7% ± 3.05) were highest ($p$ = 0.001) with chitosan, that of iron was the highest ($p$ = 0.001) with chitosan-insoluble (98.0% ± 2.6), chitosan-soluble (95.0% ± 3.60) complexes, and commercial montmorillonite clay (94.0% ± 2.3), and that of zinc (47.7% ± 3.0) was the highest ($p$ = 0.01) with the chitosan-soluble complex, and chitosan (42.66% ± 1.20) (Figure 7).

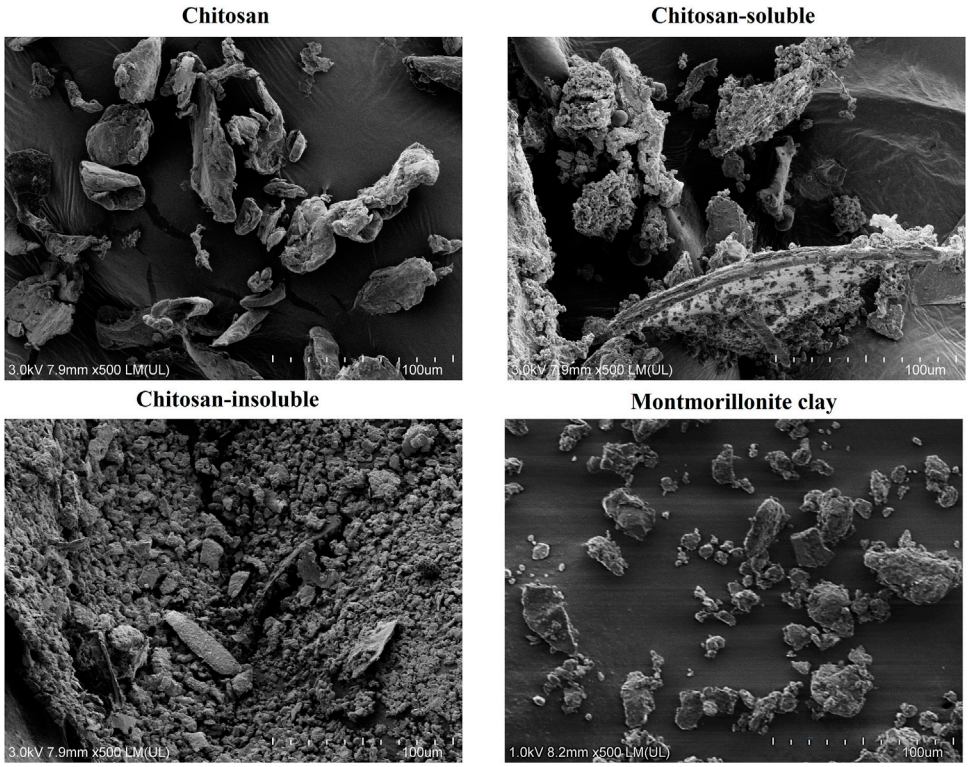


FIGURE 3
Scanning electron microscope (SEM) images of adsorbents used: chitosan, chitosan-soluble, chitosan-insoluble, and montmorillonite clay.

TABLE 2 Adsorption (%) of $AFB_1$ at different pH for chitosan, chitosan-soluble, chitosan-insoluble, and montmorillonite clay.

| Adsorbent | Percentage of $AFB_1$ (%) | | |
|---|---|---|---|
| | pH 5.2 | pH 2.5 | pH 6.6 |
| Chitosan | 17.88 ± 1.89$^c$ | 1.81 ± 0.01$^c$ | 13.05 ± 2.30$^c$ |
| Chitosan-soluble | 96.43 ± 4.72$^a$ | 38.71 ± 4.44$^b$ | 61.32 ± 2.32$^b$ |
| Chitosan-insoluble | 79.17 ± 5.15$^b$ | 72.03 ± 2.53$^a$ | 75.60 ± 3.08$^a$ |
| Montmorillonite clay | 99.40 ± 1.03$^a$ | 95.83 ± 1.03$^a$ | 82.14 ± 3.40$^a$ |

*Different letters indicate significant differences (Dunnett's test at $p \leq 0.001$), same letters show no significance difference.

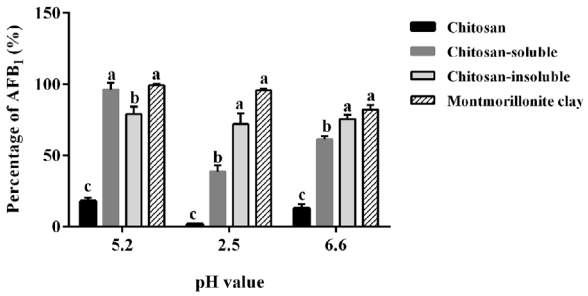


FIGURE 4
Percentage of adsorption of $AFB_1$ at different pH for chitosan, chitosan-soluble, chitosan-insoluble, and montmorillonite clay. Different letters indicate significant differences (Dunnett's test at $p \leq 0.001$), same letters show no significance difference.

# Discussion

## Adsorbent characterization *via* infrared spectroscopy

The bands of chitosan observed in the FTIR spectra are similar to those in the previous reports (Vijayalakshmi et al., 2016; Drabczyk et al., 2020). The chitosan-soluble complex was synthesized using NaOH, which deprotonates the amine groups of chitosan (observed at 1,648, and 1,564 $cm^{-1}$), thereby reducing the hydration shell and allowing the formation of new hydrogen bonds in the chitosan chain (Takara et al., 2015). The spectrum of the chitosan-insoluble complex also displayed the characteristic bands of chitosan, and the sulfate groups observed in the FTIR spectra are the result of SDS treatment and are in accordance with previous reports (Piyamongkala et al., 2008; Jiang et al., 2022).

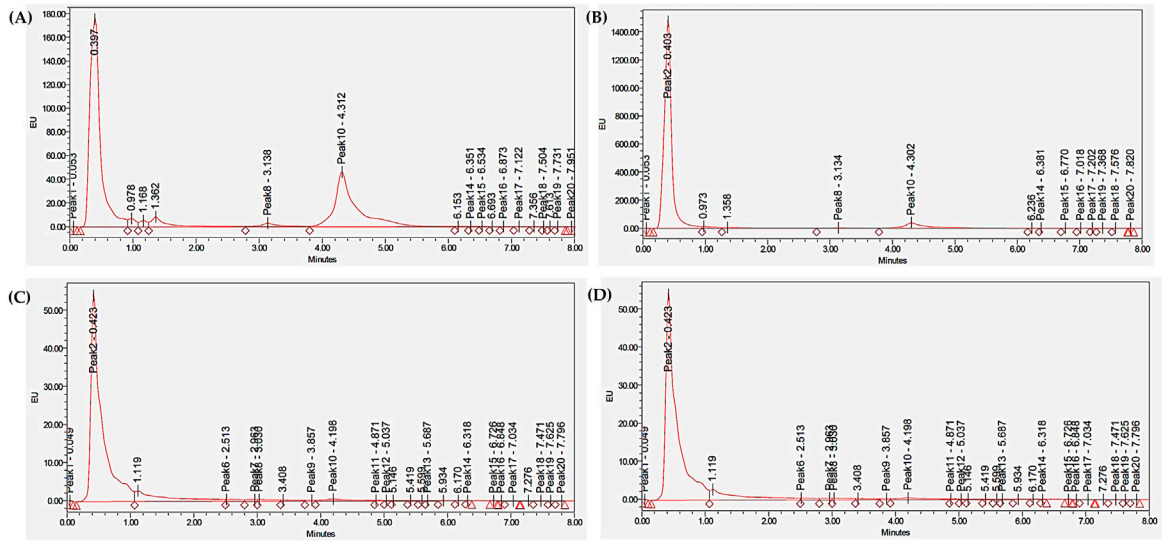


FIGURE 5
UPLC chromatograms of $AFB_1$ from the *in vitro* gastrointestinal poultry model: **(A)** chitosan, **(B)** chitosan-soluble, **(C)** chitosan-insoluble, and **(D)** montmorillonite clay.

TABLE 3 Concentration of $AFB_1$ adsorbed for chitosan, chitosan-soluble, chitosan-insoluble, and montmorillonite clay in an *in vitro* gastrointestinal poultry model.

| Adsorbent | Concentration of $AFB_1$ adsorbed (ng/ml) | Percentage of $AFB_1$ (%) |
|---|---|---|
| Control | 200 ± 0.33[a] | 0 |
| Chitosan | 117.83 ± 0.668[d] | 58.91 ± 0.334 |
| Chitosan-soluble | 129.60 ± 0.433[c] | 64.79 ± 0.217 |
| Chitosan-insoluble | 184.98 ± 0.989[b] | 93.44 ± 0.327 |
| Montmorillonite clay | 199.064 ± 0.064[a] | 99.52 ± 0.033 |

*Different letters indicate significant differences (Dunnett's test at $p \leq 0.001$), same letters show no significance difference.

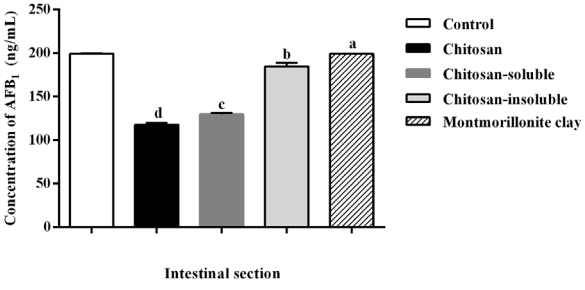


FIGURE 6
Concentration of $AFB_1$ adsorbed for chitosan, chitosan-soluble, chitosan-insoluble, and montmorillonite clay in an *in vitro* gastrointestinal poultry model. Different letters indicate significant differences (Dunnett's test at $p \leq 0.05$).

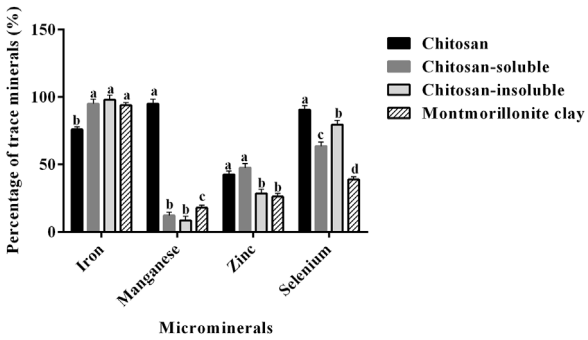


FIGURE 7
Percentage of adsorption of trace minerals for chitosan, chitosan-soluble, and chitosan-insoluble, and montmorillonite clay in an *in vitro* gastrointestinal poultry model. Different letters indicate significant differences (Dunnett's test at $p \leq 0.001$), same letters show no significance difference.

Interactions were observed between $AFB_1$ and the amine groups of chitosan and chitosan-soluble complexes and between the amine and sulfate groups in chitosan-insoluble complex. A previous study reported an electrostatic interaction within the physisorption range between a hydrogen atom (–H) of the chitosan amine group ($NH_2$) and an oxygen atom-6 (–O6) of $AFB_1$ (Juarez-Morales et al., 2018).

In the case of commercial montmorillonite clay, we observed the interaction of $AFB_1$ with silica (Si-O) and aluminum (Al-O) groups. Similarly, Desheng et al. (2005) reported that the interaction of $AFB_1$-montmorillonite clay leads to chemisorption with the

formation of double hydrogen bonds at the edge of montmorillonite clay, where the tetrahedral sheets are composed of O-Si-O (Zhou et al., 2019).

The crystalline structure of chitosan observed in the XRD patterns was in accordance with that reported in other studies (Ali et al., 2018; Morsy et al., 2019; Hao et al., 2021). The peaks of chitosan-soluble complex at 2θ = 16.76° and 18.64° are the result of treatment with sodium hydroxide (NaOH) that induces the formation of an anhydrous structure. Takara et al. (2015) observed the same effect in chitosan films treated with different concentrations of NaOH and the peaks at 2θ = 37.9° and 40.54° corresponded to the presence of sodium (Keshk and Hamdy, 2019). In the case of chitosan-insoluble complex, news peaks observed in the XRD pattern (2θ = 4.76°, 7°, and 22°) are related to the interaction of the SDS molecule with the chitosan. A similar phenomenon was observed by Jiang et al. (2022).

SEM is an analytical technique used to identify the microstructure of materials, such as size and shape (Ural, 2021). The morphology of chitosan was in accordance with that reported by Kumar and Koh (2012), in which the molecule exhibited a nonporous and crystalline morphology. However, the chitosan-soluble complex showed changes in the surface. This is consistent with previous reports that demonstrate that alkali treatment changes the polymer network producing a rough porous surface (Nakayama et al., 2020; Gültan et al., 2021). The crosslinking of chitosan with SDS generated strong intermolecular interactions shown by spherical and slightly porous structures; this result is similar to those reported in other studies (Milinković Budinčić et al., 2021; Jiang et al., 2022). We observed porous individual particles in the commercial montmorillonite clay. In contrast, Belousov et al. (2019) noticed thin leaf-shaped microaggregates with a diameter ranging from 3 to 5 to 10–20 μm. Similarly, De León et al. (2015) and Yin et al. (2016) reported a structure of plates and flat particles in montmorillonite clay.

## pH-dependent adsorption of $AFB_1$

In acidic aqueous media, the amine groups of chitosan get protonated ($NH_3^+$), and make the polymer soluble; at pH ≥ 6.5, the amine groups deprotonate to form $NH_2$, which leads to a decrease in solubility (Rinaudo, 2006). Chitosan and chitosan-soluble complexes showed lower adsorption at pH = 2.5–6.5. In contrast, the effect of pH on the performance of chitosan-insoluble complex was negligible. Treatment with NaOH results in a more soluble polymer with a lower adsorption capacity for $AFB_1$. In contrast, chitosan-insoluble complex, which is formed by the complexation of chitosan and SDS, forms highly stable physical network complexes in the pH range of 1.2–5.0 (Babak et al., 2000; Worthen et al., 2019; Miras et al., 2021). This complexation leads to the highest adsorption capacity for $AFB_1$. This result agrees with a previous report (Zhao et al., 2015), in which chitosan crosslinked with glutaraldehyde has the highest adsorption capacity for $AFB_1$, and with another report (Wang et al., 2018), in which montmorillonite modified with a surfactant nonionic has the highest affinity to $AFB_1$. Adsorption of mycotoxins involves physisorption by *Van der Waals* electrostatic interactions observed in organic binders, or chemisorption by the exchange of electrons between the adsorbent and adsorbate observed in inorganic binders (Deng et al., 2010; Di Gregorio et al., 2014; Hojati et al., 2021). Juarez-Morales et al. (2018) reported a physisorption occurring between the positive charges of amine groups of chitosan and the negative charges of the oxygen atom of $AFB_1$. The polycationic nature of chitosan allows the adsorption of polar molecules such as $AFB_1$. Desheng et al. (2005) reported an ion-dipole interaction between the carbonyl groups of $AFB_1$ and the positive ions of montmorillonite clay (Shattar et al., 2017; Li et al., 2018). These results are consistent with our results from infrared (FTIR) spectroscopy.

## Quantification of $AFB_1$ *via* UPLC in an *in vitro* gastrointestinal model for poultry

The binding capacities of adsorbents are influenced by the pH, concentration of adsorbent, enzymes, feed composition and additives, and incubation time; therefore, the stability of the adsorbent–toxin bond is important throughout the GT (Magnoli et al., 2013; Di Gregorio et al., 2014). In this study, we observed pH-dependent adsorption of $AFB_1$. The highest adsorption rates were observed with the commercial montmorillonite clay and chitosan-insoluble complex compared to the chitosan-soluble complex and chitosan. This result may be due to the high structural stability of chitosan-insoluble complexes across the different parts of the poultry GT, with an unaltered capacity of adsorption. However, Zhao et al. (2015) reported that the presence of dietary components in the GT decreased the adsorption capacity of chitosan-glutaraldehyde for $AFB_1$, and Magnoli et al. (2013) observed the same effect with sodium bentonite in presence of rumen fluid components. This effect is due to enzymes such as pepsin that can bind to the interlayers of smectites, blocking the adsorption sites for AF molecules (Barrientos-Velázquez et al., 2016). However, we did not observe differences in the adsorption capacity of $AFB_1$ for the chitosan-insoluble complex and commercial montmorillonite clay.

## Micromineral adsorption in an *in vitro* gastrointestinal model for poultry

The primary function of microminerals is to catalyze the many enzyme systems within cells (Goff, 2018). Iron takes part in oxidation-reduction reactions and its metabolism biosynthesizes hemoglobin; manganese is involved in the glycosylation of proteins, metabolism of carbohydrates and lipids, and immune function; zinc is a component of transcription proteins (Bao and Choct, 2009); and selenium is essential for normal growth and maintenance in poultry (Ševčíková et al., 2011).

Benavente (2008) observed that chitosan can adsorb metallic ions, such as copper, zinc, arsenic, and mercury, depending on the

pH, with the adsorption increasing when the pH is between four and six; meanwhile, Unagolla and Adikary (2015) reported the adsorption of cadmium and lead. Similarly, the chitosan surfactant complex has exhibited adsorption efficiency for chromium (Bat-Amgalan et al., 2021), iron, manganese (Reiad et al., 2012), and other organic (Jabeen et al., 2020) and inorganic molecules (Arumugam et al., 2019). The addition of surfactants to the chitosan polymer chain increases the adsorption capacity for diverse molecules (Matusiak et al., 2022). Similarly, clay minerals can adsorb proteins, enzymes, vitamins, and minerals (Elliott et al., 2020; Damato et al., 2022). Besides, Schlattl et al. (2021) reported that a mixture of clays such as bentonite, kaolinite, and illite adsorbed Zn, Cu, and Mn in *in vitro* conditions.

## Conclusion

Chitosan crosslinked with a surfactant molecule (SDS) was synthesized. The intramolecular interactions of the sulfate groups of SDS and the amine groups of chitosan produced a stable adsorbent at different pH values across different parts of the poultry GT *in vitro*, with greater thermal and chemical stability. In addition, this interaction generated more positively charged sites in the chitosan-insoluble complex, increasing the affinity and capacity of adsorption of $AFB_1$ (>93%), similar to the commercial clay binder. One limitation of this polymer complex, as with the commercial montmorillonite clay, in addition of adsorbing $AFB_1$, it also sequestered essential minerals. These results suggest that the chitosan-insoluble complex can be an alternative adsorbent for $AFB_1$ in poultry feed, and the next step would be an *in vivo* test.

## Data availability statement

The original contributions presented in the study are included in the article/Supplementary Material, further inquiries can be directed to the corresponding authors.

## Author contributions

SH-M, YR-Z, MF-M, and JK conceptualized this work; AD-C, SH-M, YR-Z, AM-C, and JK designed and performed the experiments; AD-C, SH-M, and AM-C analyzed the UPLC data; AD-C, SH-M, and GM-Z conducted statistical analysis; AD-C, SH-M, YR-Z, MF-M, and JK wrote the manuscript; and JK contributed to research implementation and funding acquisition.

## Funding

This study was supported by funding from the MNA de México and AQUA LAB.

## Acknowledgments

The authors gratefully acknowledge the Laboratory of Pharmacology and Toxicology (Facultad de Medicina Veterinaria y Zootecnia, Universidad Autónoma de Nuevo León) for support in processing the UPLC samples. They also thank AQUA LAB, and MNA de México for technical and financial support.

## Conflict of interest

The authors declare that the research was conducted in the absence of any commercial or financial relationships that could be construed as a potential conflict of interest.

## Publisher's note

All claims expressed in this article are solely those of the authors and do not necessarily represent those of their affiliated organizations, or those of the publisher, the editors and the reviewers. Any product that may be evaluated in this article, or claim that may be made by its manufacturer, is not guaranteed or endorsed by the publisher.

## Supplementary material

The Supplementary Material for this article can be found online at: https://www.frontiersin.org/articles/10.3389/fmats.2022.1044495/full#supplementary-material

## References

Abbasi Pirouz, A., Selamat, J., Zafar Iqbal, S., and Iskandar Putra Samsudin, N. (2020). Efficient and simultaneous chitosan-mediated removal of 11 mycotoxins from palm kernel cake. *Toxins* 12, 115. doi:10.3390/toxins12020115

Akgönüllü, S., Yavuz, H., and Denizli, A. (2020). SPR nanosensor based on molecularly imprinted polymer film with gold nanoparticles for sensitive detection of aflatoxin B1. *Talanta* 219, 121219. doi:10.1016/j.talanta.2020.121219

Ali, M. E. A., Aboelfadl, M. M. S., Selim, A. M., Khalil, H. F., and Elkady, G. M. (2018). Chitosan nanoparticles extracted from shrimp shells, application for removal of Fe(II) and Mn(II) from aqueous phases. *Sep. Sci. Technol.* 53, 2870–2881. doi:10.1080/01496395.2018.1489845

Aranaz, I., Alcántara, A. R., Civera, M. C., Arias, C., Elorza, B., Heras Caballero, A., et al. (2021). Chitosan: an overview of its properties and applications. *Polymers* 13, 3256. doi:10.3390/polym13193256

Arumugam, T. K., Krishnamoorthy, P., Rajagopalan, N. R., Nanthini, S., and Vasudevan, D. (2019). Removal of malachite green from aqueous solutions using a modified chitosan composite. *Int. J. Biol. Macromol.* 128, 655–664. doi:10.1016/j.ijbiomac.2019.01.185

Babak, V. G., Merkovich, E. A., Desbrières, J., and Rinaudo, M. (2000). Formation of an ordered nanostructure in surfactant-polyelectrolyte complexes formed by interfacial diffusion. *Polym. Bull.* 45, 77–81. doi:10.1007/s002890070059

Bao, Y. M., and Choct, M. (2009). Trace mineral nutrition for broiler chickens and prospects of application of organically complexed trace minerals: a review. *Anim. Prod. Sci.* 49, 269. doi:10.1071/EA08204

Barrientos-Velázquez, A. L., Arteaga, S., Dixon, J. B., and Deng, Y. (2016). The effects of pH, pepsin, exchange cation, and vitamins on aflatoxin adsorption on smectite in simulated gastric fluids. *Appl. Clay Sci.* 120, 17–23. doi:10.1016/j.clay.2015.11.014

Bat-Amgalan, M., Khashbaatar, Z., Anak, D. E. V., Sari, M. N. M., Miyamoto, N., Kano, N., et al. (2021). Adsorption of Cr(III) from an aqueous solution by chitosan beads modified with sodium dodecyl sulfate (SDS). *J. Environ. Prot. (Irvine, Calif.* 12, 939–960. doi:10.4236/jep.2021.1211055

Belousov, P., Semenkova, A., Egorova, T., Romanchuk, A., Zakusin, S., Dorzhieva, O., et al. (2019). Cesium sorption and desorption on glauconite, bentonite, zeolite and diatomite. *Minerals* 9, 625. doi:10.3390/min9100625

Benavente, M. (2008). Adsorption of metallic ions onto chitosan: Equlibrium and kinetic studies, Licentiate.

Bibi, I., Icenhower, J., Niazi, N. K., Naz, T., Shahid, M., and Bashir, S. (2016). "Clay minerals," in *Environmental materials and waste* (UK: Elsevier), 543–567. doi:10.1016/B978-0-12-803837-6.00021-4

Centre international de recherche sur le cancer (2002). *Some traditional herbal medicines, some mycotoxins, naphtalene and styrene* (Lyon: World health organization).

Chang, Q., Lu, Y., and Lan, R. (2020). Chitosan oligosaccharide as an effective feed additive to maintain growth performance, meat quality, muscle glycolytic metabolism, and oxidative status in yellow-feather broilers under heat stress. *Poult. Sci.* 99, 4824–4831. doi:10.1016/j.psj.2020.06.071

Chiappisi, L., and Gradzielski, M. (2015). Co-assembly in chitosan–surfactant mixtures: Thermodynamics, structures, interfacial properties and applications. *Adv. Colloid Interface Sci.* 220, 92–107. doi:10.1016/j.cis.2015.03.003

Cogliano, V. J., Baan, R., Straif, K., Grosse, Y., Lauby-Secretan, B., El Ghissassi, F., et al. (2011). Preventable exposures associated with human cancers. *JNCI J. Natl. Cancer Inst.* 103, 1827–1839. doi:10.1093/jnci/djr483

Cortés-Higareda, M., de Lorena Ramos-García, M., Correa-Pacheco, Z. N., Del Río-García, J. C., and Bautista-Baños, S. (2019). Nanostructured chitosan/propolis formulations: characterization and effect on the growth of Aspergillus flavus and production of aflatoxins. *Heliyon* 5, e01776. doi:10.1016/j.heliyon.2019.e01776

Dai, C., Tian, E., Hao, Z., Tang, S., Wang, Z., Sharma, G., et al. (2022). Aflatoxin B1 toxicity and protective effects of curcumin: Molecular mechanisms and clinical implications. *Antioxidants* 11, 2031. doi:10.3390/antiox11102031

Damato, A., Vianello, F., Novelli, E., Balzan, S., Gianesella, M., Giaretta, E., et al. (2022). Comprehensive review on the interactions of clay minerals with animal physiology and production. *Front. Vet. Sci.* 9, 889612. doi:10.3389/fvets.2022.889612

de Jesús Nava-Ramírez, M., Salazar, A. M., Sordo, M., López-Coello, C., Téllez-Isaías, G., Méndez-Albores, A., et al. (2021). Ability of low contents of biosorbents to bind the food carcinogen aflatoxin B1 *in vitro*. *Food Chem.* 345, 128863. doi:10.1016/j.foodchem.2020.128863

De León, M. A., Sergio, M., Bussi, J., Ortiz de la Plata, G. B., Cassano, A. E., and Alfano, O. M. (2015). Application of a montmorillonite clay modified with iron in photo-Fenton process. Comparison with goethite and nZVI. *Environ. Sci. Pollut. Res.* 22, 864–869. doi:10.1007/s11356-014-2681-6

Deng, Y., Velázquez, A. L. B., Billes, F., and Dixon, J. B. (2010). Bonding mechanisms between aflatoxin B1 and smectite. *Appl. Clay Sci.* 50, 92–98. doi:10.1016/j.clay.2010.07.008

Desheng, Q., Fan, L., Yanhu, Y., and Niya, Z. (2005). Adsorption of aflatoxin B1 on montmorillonite. *Poult. Sci.* 84, 959–961. doi:10.1093/ps/84.6.959

Dhanasekaran, D., Shanmugapriya, S., Thajuddin, N., and Panneerselvam, A. (2011). "Aflatoxins and aflatoxicosis in human and animals," in *Aflatoxins - biochemistry and molecular biology*. Editor R. G. Guevara-Gonzalez (London: InTechOpen). doi:10.5772/22717

Di Gregorio, M. C., Neeff, D. V. de, Jager, A. V., Corassin, C. H., Carão, Á. C. de P., Albuquerque, R. de, et al. (2014). Mineral adsorbents for prevention of mycotoxins in animal feeds. *Toxin Rev.* 33, 125–135. doi:10.3109/15569543.2014.905604

Diaz, G. J., and Murcia, H. W. (2019). An unusually high production of hepatic aflatoxin B1-dihydrodiol, the possible explanation for the high susceptibility of ducks to aflatoxin B1. *Sci. Rep.* 9, 8010. doi:10.1038/s41598-019-44515-6

Drabczyk, A., Kudłacik-Kramarczyk, S., Głąb, M., Kędzierska, M., Jaromin, A., Mierzwiński, D., et al. (2020). Physicochemical investigations of chitosan-based hydrogels containing aloe vera designed for biomedical use. *Materials* 13, 3073. doi:10.3390/ma13143073

Duan, L., Akakpo, J. Y., Ramachandran, A., and Jaeschke, H. (2019). "Environmental liver toxins," in *Encyclopedia of environmental health* (Netherland: Elsevier), 578–584. doi:10.1016/B978-0-12-409548-9.11910-4

El-Naggar, M. A., and Thabit, T. M. (2014). Evaluation of β- d- glucan biopolymer as a novel mycotoxin binder for fumonisin and deoxynivalenol in soybean feed. *Foodborne Pathogens Dis.* 11, 433–438. doi:10.1089/fpd.2013.1711

Elliott, C. T., Connolly, L., and Kolawole, O. (2020). Potential adverse effects on animal health and performance caused by the addition of mineral adsorbents to feeds to reduce mycotoxin exposure. *Mycotoxin Res.* 36, 115–126. doi:10.1007/s12550-019-00375-7

Fouad, A., Ruan, D., El-Senousey, H., Chen, W., Jiang, S., and Zheng, C. (2019). Harmful effects and control strategies of aflatoxin B1 produced by Aspergillus flavus and Aspergillus parasiticus strains on poultry: Review. *Toxins* 11, 176. doi:10.3390/toxins11030176

Goff, J. P. (2018). Invited review: Mineral absorption mechanisms, mineral interactions that affect acid–base and antioxidant status, and diet considerations to improve mineral status. *J. Dairy Sci.* 101, 2763–2813. doi:10.3168/jds.2017-13112

Guidance for FDA (2019). Action levels for aflatoxins in animal food.

Gültan, T., Bektaş Tercan, Ş., Çetin Altındal, D., and Gümüşderelioğlu, M. (2021). Synergistic effect of fabrication and stabilization methods on physicochemical and biological properties of chitosan scaffolds. *Int. J. Polym. Mater. Polym. Biomaterials* 70, 371–382. doi:10.1080/00914037.2020.1725752

Hao, G., Hu, Y., Shi, L., Chen, J., Cui, A., Weng, W., et al. (2021). Physicochemical characteristics of chitosan from swimming crab (Portunus trituberculatus) shells prepared by subcritical water pretreatment. *Sci. Rep.* 11, 1646. doi:10.1038/s41598-021-81318-0

Hojati, M., Norouzian, M. A., Assadi Alamouti, A., and Afzalzadeh, A. (2021). *In vitro* evaluation of binding capacity of different binders to adsorb aflatoxin. *Vet. Res. Forum.* 12, 211–215. doi:10.30466/vrf.2019.99431.2369

Jabeen, S., Lone, M. S., Afzal, S., Kour, P., Shaheen, A., Ahanger, F. A., et al. (2020). Effect of single and binary mixed surfactant impregnation on the adsorption capabilities of chitosan hydrogel beads toward rhodamine B. *New J. Chem.* 44, 12216–12226. doi:10.1039/D0NJ02496A

Jafari, M., Mehrnejad, F., Rahimi, F., and Asghari, S. M. (2018). The molecular basis of the sodium dodecyl sulfate effect on human ubiquitin structure: A molecular dynamics simulation study. *Sci. Rep.* 8, 2150. doi:10.1038/s41598-018-20669-7

Jiang, S., Qiao, C., Wang, X., Li, Z., and Yang, G. (2022). Structure and properties of chitosan/sodium dodecyl sulfate composite films. *RSC Adv.* 12, 3969–3978. doi:10.1039/D1RA08218C

Juarez-Morales, L. A., Hernandez-Cocoletzi, H., Chigo-Anota, E., Aguila-Almanza, E., and Tenorio-Arvide, M. G. (2018). Chitosan-aflatoxins B1, M1 interaction: A computational approach. *Curr. Org. Chem.* 21. doi:10.2174/1385272821666170511165159

Keshk, S. M. A. S., and Hamdy, M. S. (2019). Preparation and physicochemical characterization of zinc oxide/sodium cellulosecomposite for food packaging. *Turk. J. Chem.* 43, 94–105. doi:10.3906/kim-1803-83

Kim, S. W., Holanda, D. M., Gao, X., Park, I., and Yiannikouris, A. (2019). Efficacy of a yeast cell wall extract to mitigate the effect of naturally Co-occurring mycotoxins contaminating feed ingredients fed to young pigs: Impact on gut health, microbiome, and growth. *Toxins* 11, 633. doi:10.3390/toxins11110633

Kövesi, B., Cserháti, M., Erdélyi, M., Zándoki, E., Mézes, M., and Balogh, K. (2020). Lack of dose- and time-dependent effects of aflatoxin B1 on gene expression and enzymes associated with lipid peroxidation and the glutathione redox system in chicken. *Toxins* 12, 84. doi:10.3390/toxins12020084

Kumar, P., Mahato, D. K., Kamle, M., Mohanta, T. K., and Kang, S. G. (2017). Aflatoxins: A global concern for food safety, human health and their management. *Front. Microbiol.* 07, 2170. doi:10.3389/fmicb.2016.02170

Kumar, S., and Koh, J. (2012). Physiochemical, optical and biological activity of chitosan-chromone derivative for biomedical applications. *Int. J. Mol. Sci.* 13, 6102–6116. doi:10.3390/ijms13056102

Kumari, N., and Mohan, C. (2021). "Basics of clay minerals and their characteristic properties," in *Clay and clay minerals*. Editor G. Morari Do Nascimento (UK: IntechOpen). doi:10.5772/intechopen.97672

Kurup, A. H., Patras, A., Pendyala, B., Vergne, M. J., and Bansode, R. R. (2022). Evaluation of ultraviolet-light (UV-A) emitting diodes technology on the reduction of spiked aflatoxin B1 and aflatoxin M1 in whole milk. *Food bioproc. Tech.* 15, 165–176. doi:10.1007/s11947-021-02731-x

Li, P., and Ishiguro, M. (2016). Adsorption of anionic surfactant (sodium dodecyl sulfate) on silica. *Soil Sci. Plant Nutr.* 62, 223–229. doi:10.1080/00380768.2016.1191969

Li, Y., Tian, G., Dong, G., Bai, S., Han, X., Liang, J., et al. (2018). Research progress on the raw and modified montmorillonites as adsorbents for mycotoxins: A review. *Appl. Clay Sci.* 163, 299–311. doi:10.1016/j.clay.2018.07.032

Liew, W.-P.-P., and Mohd-Redzwan, S. (2018). Mycotoxin: Its impact on gut health and microbiota. *Front. Cell. Infect. Microbiol.* 8, 60. doi:10.3389/fcimb.2018.00060

Luo, Y., Liu, X., Yuan, L., and Li, J. (2020). Complicated interactions between bio-adsorbents and mycotoxins during mycotoxin adsorption: Current research and future prospects. *Trends Food Sci. Technol.* 96, 127–134. doi:10.1016/j.tifs.2019.12.012

Magnoli, A. P., Alonso, V. A., Cavaglieri, L. R., Dalcero, A. M., and Chiacchiera, S. M. (2013). Effect of monogastric and ruminant gastrointestinal conditions on *in vitro* aflatoxin $B_1$ adsorption ability by a montmorillonite. *Food Addit. Contam. Part A* 30, 743–749. doi:10.1080/19440049.2013.784398

Marchese, S., Polo, A., Ariano, A., Velotto, S., Costantini, S., and Severino, L. (2018). Aflatoxin B1 and M1: Biological properties and their involvement in cancer development. *Toxins* 10, 214. doi:10.3390/toxins10060214

Marroquín-Cardona, A., Deng, Y., Taylor, J. F., Hallmark, C. T., Johnson, N. M., and Phillips, T. D. (2009). *In vitro* and *in vivo* characterization of mycotoxin-binding additives used for animal feeds in Mexico. *Food Addit. Contam. Part A* 26, 733–743. doi:10.1080/02652030802641872

Matusiak, J., Grządka, E., Maciołek, U., Godek, E., and Guzmán, E. (2022). The journey of tuning chitosan properties in colloidal systems: Interactions with surfactants in the bulk and on the alumina surface. *Chem. Eng. J.* 450, 138145. doi:10.1016/j.cej.2022.138145

McKenzie, K. S., Kubena, L. F., Denvir, A. J., Rogers, T. D., Hitchens, G. D., Bailey, R. H., et al. (1998). Aflatoxicosis in Turkey poults is prevented by treatment of naturally contaminated corn with ozone generated by electrolysis. *Poult. Sci.* 77, 1094–1102. doi:10.1093/ps/77.8.1094

Milinković Budinčić, J., Petrović, L., Đekić, L., Aleksić, M., Fraj, J., Popović, S., et al. (2021). Chitosan/sodium dodecyl sulfate complexes for microencapsulation of vitamin E and its release profile—understanding the effect of anionic surfactant. *Pharmaceuticals* 15, 54. doi:10.3390/ph15010054

Miras, J., Liu, C., Blomberg, E., Thormann, E., Vílchez, S., and Esquena, J. (2021). pH-responsive chitosan nanofilms crosslinked with genipin. *Colloids Surfaces A Physicochem. Eng. Aspects* 616, 126229. doi:10.1016/j.colsurfa.2021.126229

Morsy, M., Mostafa, K., Amyn, H., El-Ebissy, A., Salah, A., and Youssef, M. (2019). Synthesis and characterization of freeze dryer chitosan nano particles as multi functional eco-friendly finish for fabricating easy care and antibacterial cotton textiles. *Egypt. J. Chem.* 0, 0. doi:10.1010.21608/ejchem.2019.6995.1583

Muxika, A., Etxabide, A., Uranga, J., Guerrero, P., and de la Caba, K. (2017). Chitosan as a bioactive polymer: Processing, properties and applications. *Int. J. Biol. Macromol.* 105, 1358–1368. doi:10.1016/j.ijbiomac.2017.07.087

Nakayama, R., Katsumata, K., Niwa, Y., and Namiki, N. (2020). Dependence of water-permeable chitosan membranes on chitosan molecular weight and alkali treatment. *Membranes* 10, 351. doi:10.3390/membranes10110351

Neeff, D. V., Carão, A. C. P., Gonçalves, B. L., Bordin, K., Corassin, C. H., Ledoux, D. R., et al. (2018). Natural antioxidants as detoxifying agents for aflatoxins in animal feed. *Anim. Nutr. Feed Tech.* 18, 281. doi:10.5958/0974-181X.2018.00027.6

Nuengjamnong, C., and Angkanaporn, K. (2018). Efficacy of dietary chitosan on growth performance, haematological parameters and gut function in broilers. *Italian J. Animal Sci.* 17, 428–435. doi:10.1080/1828051X.2017.1373609

Núnez-Delgado, A. (2021). *Sorbents materials for controlling environmental pollution: current state and trends* (Amsterdam KidlingtonOxford Cambridge, MA: Elsevier)

Ochieng, P. E., Scippo, M.-L., Kemboi, D. C., Croubels, S., Okoth, S., Kang'ethe, E. K., et al. (2021). Mycotoxins in poultry feed and feed ingredients from sub-saharan africa and their impact on the production of broiler and layer chickens: A review. *Toxins* 13, 633. doi:10.3390/toxins13090633

Odom, I. E. (1984). Smectite clay minerals: properties and uses. *Phil. Trans. R. Soc. Lond. A* 311, 391–409. doi:10.1098/rsta.1984.0036

Omotayo, O. P., Omotayo, A. O., Mwanza, M., and Babalola, O. O. (2019). Prevalence of mycotoxins and their consequences on human health. *Toxicol. Res.* 35, 1–7. doi:10.5487/TR.2019.35.1.001

Omur, A. D., Yildirim, B., Saglam, Y. S., Comakli, S., and Ozkaraca, M. (2019). Activity of resveratrol on the influence of aflatoxin B1 on the testes of Sprague dawley rats. *Pol. J. Vet. Sci.* 22, 313–320. doi:10.24425/PJVS.2019.129222

Osho, S. O., and Adeola, O. (2019). Impact of dietary chitosan oligosaccharide and its effects on coccidia challenge in broiler chickens. *Br. Poult. Sci.* 60, 766–776. doi:10.1080/00071668.2019.1662887

Patrick, B. N., and Stepman, F. (2019). Mycotoxins - impact and management strategies. InTech Available at: http://resolver.ebscohost.com/Redirect/PRL?EPPackageLocationID=4377.23138053.54857329&epcustomerid=s8491974&db=4377 [Accessed July 8, 2022].

Pauletto, M., Giantin, M., Tolosi, R., Bassan, I., Barbarossa, A., Zaghini, A., et al. (2021). Discovering the protective effects of resveratrol on aflatoxin B1-induced toxicity: A whole transcriptomic study in a bovine hepatocyte cell line. *Antioxidants* 10, 1225. doi:10.3390/antiox10081225

Peles, F., Sipos, P., Győri, Z., Pfliegler, W. P., Giacometti, F., Serraino, A., et al. (2019). Adverse effects, transformation and channeling of aflatoxins into food raw materials in livestock. *Front. Microbiol.* 10, 2861. doi:10.3389/fmicb.2019.02861

Petrovic, L., Milinkovic, J., Fraj, J., Bucko, S., and Katona, J. (2016). An investigation of chitosan and sodium dodecyl sulfate interactions in acetic media. *J. Serb Chem. Soc.* 81, 575–587. doi:10.2298/JSC151119024P

Piyamongkala, K., Mekasut, L., and Pongstabodee, S. (2008). Cutting fluid effluent removal by adsorption on chitosan and sds-modified chitosan. *Macromol. Res.* 16, 492–502. doi:10.1007/BF03218550

M. N. V. Prasad, M. Vithanage, and A. Kapley (Editors) (2019). *Pharmaceuticals and personal care products: waste management and treatment technology: emerging contaminants and micro pollutants* (Oxford, United Kingdom ; Cambridge, MA, United States: Butterworth-Heinemann is an imprint of Elsevier).

Razzaghi-Abyaneh, M. (2013). Aflatoxins - recent advances and future prospects. Available at: https://www.doabooks.org/doab?func=fulltext&uiLanguage=en&rid=36454 [Accessed July 8, 2022].

Reiad, N. A., Salam, O. E. A., Abadir, E. F., and Harraz, F. A. (2012). Adsorptive removal of iron and manganese ions from aqueous solutions with microporous chitosan/polyethylene glycol blend membrane. *J. Environ. Sci.* 24, 1425–1432. doi:10.1016/S1001-0742(11)60954-6

Rinaudo, M. (2006). Chitin and chitosan: Properties and applications. *Prog. Polym. Sci.* 31, 603–632. doi:10.1016/j.progpolymsci.2006.06.001

Ross Broiler: Nutrition Specifications (2019). Ross broiler: Nutrition Specifications. Available at: https://en.aviagen.com/assets/Tech_Center/Ross_Broiler/RossBroilerNutritionSpecs2019-EN.pdf.

Salvador, J.-P., Vasylieva, N., Gonzalez-Garcia, I., Jin, M., Caster, R., Siegel, J. B., et al. (2022). Nanobody-based lateral flow immunoassay for the rapid detection of aflatoxin B1 in almond milk. *ACS Food Sci. Technol.* 2, 1276–1282. doi:10.1021/acsfoodscitech.2c00118

Schlattl, M., Buffler, M., and Windisch, W. (2021). Clay minerals affect the solubility of Zn and other bivalent cations in the digestive tract of ruminants *in vitro*. *Animals* 11, 877. doi:10.3390/ani11030877

Segura-Palacios, M. A., Correa-Pacheco, Z. N., Corona-Rangel, M. L., Martinez-Ramirez, O. C., Salazar-Piña, D. A., Ramos-García, M. de L., et al. (2021). Use of natural products on the control of Aspergillus flavus and production of aflatoxins *in vitro* and on tomato fruit. *Plants* 10, 2553. doi:10.3390/plants10122553

Ševčíková, S., Skřivan, M., Dlouhá, G., and Koucký, M. (2011). The effect of selenium source on the performance and meat quality of broiler chickens. *Czech J. Anim. Sci.* 51, 449–457. doi:10.17221/3964-CJAS

Shattar, S. F. A., Zakaria, N. A., and Foo, K. Y. (2017). Utilization of montmorillonite as a refining solution for the treatment of ametryn, a second generation of pesticide. *J. Environ. Chem. Eng.* 5, 3235–3242. doi:10.1016/j.jece.2017.06.031

Sid, S., Mor, R. S., Kishore, A., and Sharanagat, V. S. (2021). Bio-sourced polymers as alternatives to conventional food packaging materials: A review. *Trends Food Sci. Technol.* 115, 87–104. doi:10.1016/j.tifs.2021.06.026

Solís-Cruz, B., Hernández-Patlán, D., Beyssac, E., Latorre, J., Hernandez-Velasco, X., Merino-Guzman, R., et al. (2017). Evaluation of chitosan and cellulosic polymers as binding adsorbent materials to prevent aflatoxin B1, fumonisin B1, ochratoxin, trichothecene, deoxynivalenol, and zearalenone mycotoxicoses through an *in vitro* gastrointestinal model for poultry. *Polymers* 9, 529. doi:10.3390/polym9100529

Speight, J. G. (2020). "Thermodynamics of water," in *Natural water remediation* (Netherland: Elsevier), 131–163. doi:10.1016/B978-0-12-803810-9.00004-8

Su, Q.-Y. (2020). "The toxification and detoxification mechanisms of aflatoxin B1 in human: An update," in *Aflatoxin B1 occurrence, detection and toxicological effects*. Editor X.-D. Long (UK: IntechOpen). doi:10.5772/intechopen.89221

Swiatkiewicz, S., Swiatkiewicz, M., Arczewska-Wlosek, A., and Jozefiak, D. (2015). Chitosan and its oligosaccharide derivatives (chito-oligosaccharides) as

feed supplements in poultry and swine nutrition. *J. Anim. Physiol. Anim. Nutr. Berl.* 99, 1–12. doi:10.1111/jpn.12222

Takara, E. A., Marchese, J., and Ochoa, N. A. (2015). NaOH treatment of chitosan films: Impact on macromolecular structure and film properties. *Carbohydr. Polym.* 132, 25–30. doi:10.1016/j.carbpol.2015.05.077

Tozzi, B., Liponi, G. B., Meucci, V., Casini, L., Dall'Asta, C., Intorre, L., et al. (2016). Aflatoxins M1 and M2 in the milk of donkeys fed with naturally contaminated diet. *Dairy Sci. Technol.* 96, 513–523. doi:10.1007/s13594-016-0285-2

Unagolla, J. M., and Adikary, S. U. (2015). "Adsorption of cadmium and lead heavy metals by chitosan biopolymer: A study on equilibrium isotherms and kinetics," in 2015 Moratuwa Engineering Research Conference (MERCon) (Moratuwa, Sri Lanka: IEEE), Srilanka, Apr 7-8, 234–239. doi:10.1109/MERCon.2015.7112351

Ural, N. (2021). The significance of scanning electron microscopy (SEM) analysis on the microstructure of improved clay: An overview. *Open Geosci.* 13, 197–218. doi:10.1515/geo-2020-0145

Vijayalakshmi, K., Devi, B. M., and Sudha, P. N. (2016). Synthesis, characterization and applications of nanochitosan/sodium alginate/microcrystalline cellulose film. *J. Nanomed. Nanotechnol.* 07. doi:10.4172/2157-7439.1000419

Vakili, M., Deng, S., Cagnetta, G., Wang, W., Meng, P., Liu, D., et al. (2019). Regeneration of chitosan-based adsorbents used in heavy metal adsorption: A review. *Sep. Purif. Technol.* 224, 373–387. doi:10.1016/j.seppur.2019.05.040

Wang, G., Lian, C., Xi, Y., Sun, Z., and Zheng, S. (2018). Evaluation of nonionic surfactant modified montmorillonite as mycotoxins adsorbent for aflatoxin B1 and zearalenone. *J. Colloid Interface Sci.* 518, 48–56. doi:10.1016/j.jcis.2018.02.020

Wang, W., Meng, Q., Li, Q., Liu, J., Zhou, M., Jin, Z., et al. (2020). Chitosan derivatives and their application in biomedicine. *Int. J. Mol. Sci.* 21, 487. doi:10.3390/ijms21020487

Wang, X., Wang, T., Nepovimova, E., Long, M., Wu, W., and Kuca, K. (2022). Progress on the detoxification of aflatoxin B1 using natural anti-oxidants. *Food Chem. Toxicol.* 169, 113417. doi:10.1016/j.fct.2022.113417

Worthen, A., Irving, K., and Lapitsky, Y. (2019). Supramolecular strategy effects on chitosan bead stability in acidic media: A comparative study. *Gels* 5, 11. doi:10.3390/gels5010011

Wu, J., Gan, Z., Zhuo, R., Zhang, L., Wang, T., and Zhong, X. (2020). Resveratrol attenuates aflatoxin B1-induced ROS formation and increase of m6A RNA methylation. *Animals* 10, 677. doi:10.3390/ani10040677

Wu, K., Liu, M., Wang, H., Rajput, S. A., Shan, Y., Qi, D., et al. (2021). The mechanism underlying the extreme sensitivity of duck to aflatoxin B1. *Oxidative Med. Cell. Longev.* 2021, 1–8. doi:10.1155/2021/9996503

Yadav, N., Yadav, S. S., Chhillar, A. K., and Rana, J. S. (2021). An overview of nanomaterial based biosensors for detection of Aflatoxin B1 toxicity in foods. *Food Chem. Toxicol.* 152, 112201. doi:10.1016/j.fct.2021.112201

Yang, J., Bai, F., Zhang, K., Lv, X., Bai, S., Zhao, L., et al. (2012). Effects of feeding corn naturally contaminated with $AFB_1$ and $AFB_2$ on performance and aflatoxin residues in broilers. *Czech J. Anim. Sci.* 57, 506–515. doi:10.17221/6383-CJAS

Yin, X., Xie, X., Wu, X., and An, X. (2016). Catalytic performance of nickel immobilized on organically modified montmorillonite in the steam reforming of ethanol for hydrogen production. *J. Fuel Chem. Technol.* 44, 689–697. doi:10.1016/S1872-5813(16)30033-0

Zachetti, V., Cendoya, E., Nichea, M., Chulze, S., and Ramirez, M. (2019). Preliminary study on the use of chitosan as an eco-friendly alternative to control Fusarium growth and mycotoxin production on maize and wheat. *Pathogens* 8, 29. doi:10.3390/pathogens8010029

Zavala-Franco, A., Hernández-Patlán, D., Solís-Cruz, B., López-Arellano, R., Tellez-Isaias, G., Vázquez-Durán, A., et al. (2018). Assessing the aflatoxin B1 adsorption capacity between biosorbents using an *in vitro* multicompartmental model simulating the dynamic conditions in the gastrointestinal tract of poultry. *Toxins* 10, 484. doi:10.3390/toxins10110484

Zhao, D., Yu, S., Sun, B., Gao, S., Guo, S., and Zhao, K. (2018). Biomedical applications of chitosan and its derivative nanoparticles. *Polymers* 10, 462. doi:10.3390/polym10040462

Zhao, Z., Liu, N., Yang, L., Wang, J., Song, S., Nie, D., et al. (2015). Cross-linked chitosan polymers as generic adsorbents for simultaneous adsorption of multiple mycotoxins. *Food control.* 57, 362–369. doi:10.1016/j.foodcont.2015.05.014

Zhou, C., Tong, D., and Yu, W. (2019). "Smectite nanomaterials: Preparation, properties, and functional applications," in *Nanomaterials from clay minerals* (Netherland: Elsevier), 335–364. doi:10.1016/B978-0-12-814533-3.00007-7